

# CONTINUUM DAMAGE MECHANICS MODELING OF THE FAILURE OF REFRACTORY CUP UNDER THERMAL LOADING AND CHEMICAL SHRINKAGE

Xiaoting Liang<sup>1</sup>, William L. Headrick<sup>2</sup>, Lokeswarappa R. Dharani<sup>3</sup>

<sup>1</sup>Postdoctoral fellow, Department of Materials Science and Engineering, University of Missouri-Rolla, MO 65409-0330

<sup>2</sup>Assistant Research Professor, Department of Materials Science and Engineering, University of Missouri-Rolla, MO 65409-0330, Phone: (573) 341-4188 E-mail: [bill@umr.edu](mailto:bill@umr.edu)

<sup>3</sup>Curators' Professor, Department of Mechanical and Aerospace Engineering, University of Missouri-Rolla, MO 65409-0050

## ABSTRACT

Refractories are widely used in the glass-making, steel-making and energy-production industries in which they are subjected to significant thermal loading and chemical attack. As brittle material, refractory failure under thermal loading and chemical attack is usually caused by the formation of micro-cracks. Continuum damage mechanics (CDM) based model has been attempted previously to reflect the influence of the micro-crack formation on the failure of a refractory cup experiencing thermal and chemical expansion. Chemical reaction was found to be the dominant factor of the failure of the refractory cup. In order to further understand the effect of the chemical reaction, a CDM based model is developed to simulate the failure behavior of a refractory cup with shrinkage due to the chemical reaction. This work would help understanding the failure behavior of refractories exposed to high temperature and corrosive environments, therefore helping in the development and application of refractories.

## INTRODUCTION

Refractories are widely used for the linings of furnaces and vessels of the glass-making, steel-making and energy-production industries. However, refractory linings in these applications are usually subjected to high temperature and chemical attack, resulting in volume change and strength degradation, which lead to cracking [1-6]. Since it is very hard and costly to study the failure behavior of refractories experimentally due to the high temperature and the corrosion environment, computer modeling has been applied to study the thermomechanical behavior of refractories extensively [7-14]. However, due to brittle behavior of refractories, the failure of refractories is caused by the formation of micro-cracks. The traditional thermomechanical modeling is not sufficient to study the failure behavior of refractories due to the formation of micro-cracks. A continuum damage mechanics (CDM) based model has been attempted previously to reflect the influence of the micro-crack formation

on the failure of a refractory cup experiencing thermal and chemical expansion [15]. The modeling provided an efficient way for thorough understanding of the failure of refractory under thermal loading and chemical attack. Chemical reaction was found to be the dominant factor of the failure of the refractory cup.

In order to further understand the effect of the chemical reaction, a CDM based model is developed to simulate the failure behavior of a refractory cup with shrinkage due to the chemical reaction.

## CONTINUUM DAMAGE MECHANICS

Refractories are classified as brittle materials. The failure of refractories due to thermal loading and corrosion is usually represented by the formation of micro-cracks. Due to the difficulties in describing the evolution of the micro-crack pattern in a failing brittle solid, continuum damage mechanics (CDM) has been used extensively to describe the failure processes of brittle materials such as concrete, rock and glass.

CDM, regarded as a continuous measurement of internal stiffness degradation of a material, was first introduced by Kachanov [16] and further developed by Lemaitre [17], Kachanov [18], and Chaboche [19]. The general purpose of CDM is to describe the coupling effects of damage process and the stress-strain behavior of a material. The effect of damage on the deformation processes is taken into account by introducing damage variables into the constitutive equations of the continuum. Instead of trying to reproduce the fine details of the micro-defect and macro-crack patterns, CDM attempts to formulate a theory that will reflect the influence of these defects in a brittle solid in an approximate manner. A scalar variable,  $D$ , between 0 and 1 is used to describe the damage. The constitutive law for a damaged material was derived by using the effective stress, along with the principle of strain equivalence. The damage variable is described in terms of stiffnesses as

$$D = 1 - \frac{\tilde{E}}{E} \quad (1)$$

where  $\tilde{E}$  is the effective elastic modulus of the material, and  $E$  is the elastic modulus of the undamaged material. The effective stress in a damaged material under uniaxial load can be expressed as:

$$\tilde{\sigma} = \frac{\sigma}{1-D} \quad (2)$$

where  $\sigma$  is the normal stress. Failure is defined as when  $D$  reaches the critical damage. The concept of failure here represents the formation of macroscopic defects rather than rupture.

Hillerborg, et al. [20] studied the tensile behavior of concrete and described a method that explains both the growth of existing cracks and the formation of new cracks. A fictitious-crack model was proposed by him based on plasticity theory. The formation and propagation of cracks was assumed to start when the tensile stress reaches a critical value. A plastic-damage model was introduced by Lubliner, et al. [21] to govern the non-linear behavior of concrete, including failure, in both tension and compression. The model was further developed by Lee and Fenves [22]. In this model, isotropic damage variables were used to represent the degradation of elastic stiffness. Uniaxial tensile and compressive stresses were expressed in terms of tensile and compressive damages and effective-stress responses. The effective stress was related to the damaged elastic stiffness and the elastic strain. The plastic strain rate was evaluated by a flow rule, using a scalar plastic potential function.

Saetta, et al. [23] studied the mechanical behavior of concrete under physical-chemical attacks by using a coupled mechanical and chemical damage model. The mechanical damage variable was defined as the ratio between the area occupied by the voids and the overall section area.

$$D_{mech} = 1 - \frac{\tilde{S}}{S} \quad (3)$$

where  $\tilde{S}$  is the effective resisting area of the damaged material and  $S$  is the overall section. The continuously decreasing manner of the effective resisting area determined that the damage variable is an increasing parameter.

The chemical damage is defined by the following relationship:

$$D_{mech} = (1 - \varphi) - \frac{1 - \varphi}{1 + (2R)^4} \quad (4)$$

where coefficient  $\varphi$  is the relative residual strength of the material achieved when the chemical reaction is completely developed. Parameter  $R$  is defined as the ratio between the actual concentration and the reference concentration of the pollutant,  $C/C_{ref}$ .

By combining the mechanical and chemical damage, the coupled damage is introduced as:

$$D_{coupled} = 1 - (1 - D_{mech}) \cdot (1 - D_{chem}) \quad (5)$$

The constitutive damage model of the material is defined as:

$$\sigma_{ij} = (1 - D_{coupled}) \cdot E_{ijkl}^0 \quad (6)$$

where  $\sigma_{ij}$  and  $\varepsilon_{ij}$  are the standard stress and strain tensors;  $E_{ijkl}^0$  is the elastic constitutive tensor and  $D$  is the mechanical damage index.

Zhao [24] developed a damage model for a laminated glass impacted by head form based on a linear damage evolution law. Damage components were defined linearly related with the corresponding tensile principal stress and maximum shear stress components. The model gave the amount of the damage of glass plies as well as the damage modes.

Liang [25] developed an inelastic-damage model for a cylindrical refractory lining under thermal loading and chemical attack. Two damage variables were used to describe the tensile and compressive damages of the refractory linings, respectively. They were defined to be functions of the inelastic strains and temperature. The total strain was defined as the sum of the mechanical strain, thermal strain and reactive strain. The chemical reaction of refractory material was expressed by the reactive strain which is a function of the temperature and time. The comparison of the predicted damage patterns and observed damage patterns in a brick from an oxy-fuel glass tank was encouraging.

## DAMAGE MODEL FOR REFRACTORY CUP

The refractory cup and the cup test procedure are taken as same as those in the study of Liang et al. [15]. The diameter of the refractory cup is 114.3 mm, the inner radius of the cup is 19.05 mm, the thickness of the cup is 76.2 mm and the depth of hole is 38.1 mm, as shown in **Figure 1**. The



**Figure 1.** A refractory cup after corrosion test.

refractory cup was set in a box furnace flooded with Argon gas. 50 g black liquor smelt was put into the cup. The temperature in the furnace was increased from room temperature to 1000°C with a heating rate of 1°C/min and then the temperature was held constant for 240 hours. Then the furnace was cooled down to room temperature at a cooling rate of 1°C/min. After the test, the refractory cup was cut apart for the corrosion and failure analysis.

The idealized geometry of the refractory cup used in the model is shown in **Figure 2**. The outer radius of the refractory cup is 57 mm, the inner radius of the cup is 19 mm, the thickness of the cup is 76 mm and the depth of hole is 38 mm.

## COUPLED THERMOMECHANICAL MODEL

The refractory material is considered as a homogeneous isotropic thermoelastic material. The coupled governing thermoelastic equations in time domain are written as [26]

$$(kT_{,i})_{,i} + Q_i + \beta_{ij} T \varepsilon_{ij}^e = \rho C \dot{T}, \quad (i, j = 1, 2, 3) \quad (7)$$

where  $k$  is the conductivity,  $T$  is the temperature,  $Q$  is the heat flow rate,  $\beta_{ij} T \varepsilon_{ij}^e$  is the thermoelastic coupling factor,  $\rho$  is the density, and  $C$  is the specific heat. According to the Fourier law of heat conduction,  $(kT_{,i})_{,i} + q_{i,i}$  in which  $q_i$  is the heat flux.

## CONSTITUTIVE RELATIONS

In modeling the cracking behavior of the refractory material, the refractory is modeled as an isotropic elastic material. After including the chemical shrinkage in the stress-strain relations for the refractory, the elastic constitutive relations for the refractory material become

$$\varepsilon_{ij} = \frac{(1+\nu)}{\tilde{E}} \left( \sigma_{ij} - \frac{\nu}{1+\nu} S_{kk} \delta_{ij} \right) + \alpha T \delta_{ij} + \varepsilon^r \delta_{ij} \quad (8)$$

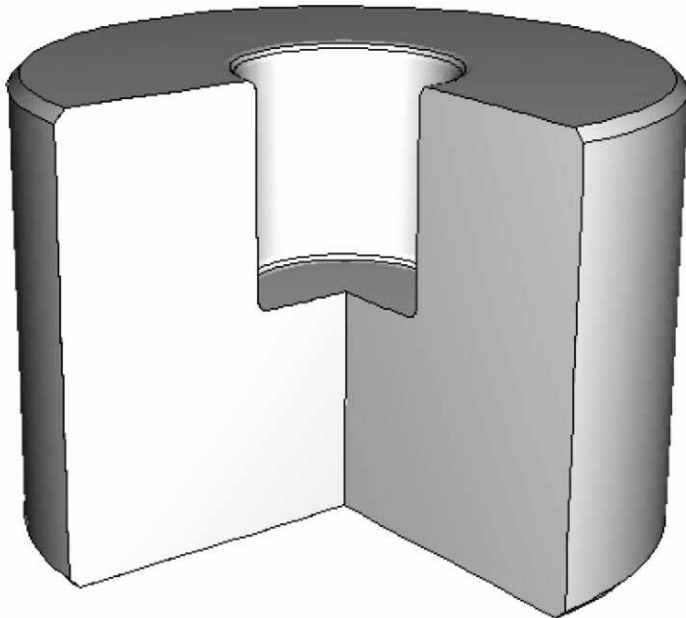


**Figure 2.** A cut-away view of the idealized refractory cup modeled.

where  $\nu$  is the Poisson's ratio,  $\alpha$  is the coefficient of thermal expansion,  $T$  is the temperature,  $\varepsilon^r$  is the chemical shrinkage strain, and  $\delta_{ij}$  is the Kronecker delta.

The chemical reaction of refractory material is controlled by temperature, time and the depth of penetration. Reactive strain is used to describe the chemical reaction as a function of the temperature,  $T$ , time,  $t$ , and penetration depth,  $d$ .

$$\varepsilon^r = F(T, t, d) \quad (9)$$

## DAMAGE MODEL

Since the failure behaviors of refractories under tension and compression are different, two damage variables,  $D$  and  $D_c$ , are used to describe the tensile and compressive damages of the refractory. The damage components due to normal principal stresses are assumed to follow a simple linear damage evolution law in which damage is linearly related with the corresponding tensile and compressive principal stress components ( $\sigma_i$ ) in a certain stress range [24]:

$$\begin{aligned} D_i &= 0, & \text{if } \sigma_i \leq \sigma_{threshold} \\ D_i &= \frac{\sigma_i - \sigma_{threshold}}{\sigma_{crit} - \sigma_{threshold}} & \text{if } \sigma_{threshold} < \sigma_i < \sigma_{crit} \\ D_i &= 1, & \text{if } \sigma_i \geq \sigma_{crit} \end{aligned} \quad (10)$$

where  $i = 1, 2$  which represent tensile and compressive, respectively.

The material degradation is modeled by loss of stiffness as

$$\tilde{E} = (1-D)E \quad (11)$$

where the total damage,  $D$ , is the combination of the tensile and compressive damages.

$$D = 1 - (1-D_t) \cdot (1-D_c) \quad (12)$$

## COMPUTATIONAL MODEL

A 2-D axisymmetric coupled temperature-displacement finite element model is used to simulate the refractory cup under thermal loading and chemical attack. The coupling of the thermal and mechanical behavior is achieved in the following matrix:

$$\begin{bmatrix} K_{UU} & K_{UT} \\ K_{TU} & K_{TT} \end{bmatrix} \begin{bmatrix} \Delta U \\ \Delta T \end{bmatrix} = \begin{Bmatrix} R_U \\ R_T \end{Bmatrix} \quad (13)$$

where  $\Delta U$  is the incremental displacement including both thermal and chemical shrinkages if involved,  $\Delta T$  is the incremental temperature,  $K_{ij}$  are submatrices of the fully coupled Jacobian matrix, and  $R_U$  and  $R_T$  are the mechanical and thermal residual vectors, respectively.

The commercial finite element package ABAQUS [27] is used for the modeling. The refractory cup is modeled with four-node bilinear axisymmetric elements CAX4RT. After performing a mesh sensitivity study, a finer mesh is employed in the possible reaction

region in order to better capture the damage state of the refractory cup, as shown in **Figure 3**.

A FORTRAN language programmed user material subroutine UMAT [27] is developed and implemented to interface with the main ABAQUS code to simulate the constitutive behavior of the refractory using the CDM approach described earlier. For a given material point, the magnitude of the damage tensor ranges from 0.0 (virgin state) to 1.0 (fully damaged state or visible cracking). The elastic modulus of the material point degrades according to equation (11). Because of the irreversibility of the damage process, the components for the damage tensor at the  $n^{\text{th}}$  time increment are determined from the current and previous state using the relationship:

$$D_i^n = \max(D_i^n, D_i^{n-1}) \quad (14)$$

where  $n$  and  $n-1$  represent the  $n^{\text{th}}$  and the  $(n-1)^{\text{th}}$  time increment in the analysis.

Due to the unavailable data of the properties of the tested material, the properties of an alumina refractory material is employed in this model. Some temperature dependent properties of the refractory are given in **Table 1**. Other properties of the refractory are described below.  $E = 103$  GPa at  $23^\circ\text{C}$  and  $E = 77$  GPa at  $1000^\circ\text{C}$ , the Young's modulus at other temperatures will be linearly interpolated based on the above two values. The following properties of the refractory are at room temperature:  $\rho = 3480$  kg/m<sup>3</sup>,  $\alpha = 8.7 \times 10^{-6}/\text{K}$  and  $\nu = 0.24$ .

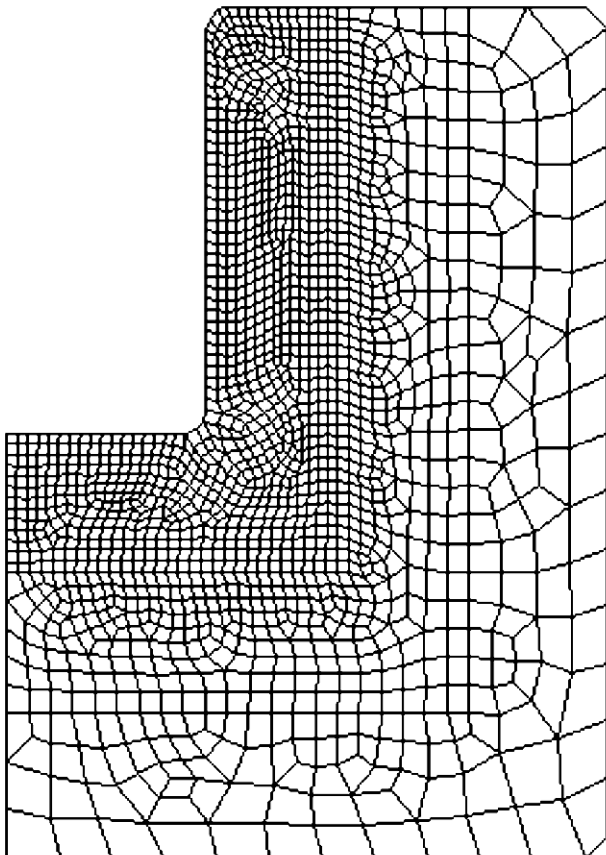


**Figure 3.** Illustration of the model and mesh.

**Table 1. Temperature dependent properties of refractory used in the model**

Temperature (°C)	Thermal conductivity (W/m K)	Specific heat (J/kg K)
23	9.34	778
100	9.28	916
200	8.29	1010
300	7.55	1080
400	6.75	1130
500	5.81	1170
600	4.37	1210
700	4.65	1220
800	4.76	1240
900	4.86	1250
1000	5.21	1270

Compressive and tensile strengths of alumina refractories at ambient temperature can reach about 3000 MPa and about 200 MPa [28, 29], respectively. However, it is well known that the strength of refractory materials would be decreased dramatically when exposed to high temperature and chemical corrosion environments. In the model, the threshold compressive and tensile strengths are assumed to be 50 MPa and 10 MPa, respectively. The critical compressive and tensile strengths are assumed to be 300 MPa and 100 MPa as the damage criterion of the refractory material, respectively, due to the paucity of knowledge on the strength of refractories under such environments.

Since there is no experimental data on the reaction rate, assumptions have been made for the reaction rate based on the study of Peascoe et al. [30]. The chemical reaction is assumed to occur only when temperature is above  $800^\circ\text{C}$ . A constant expansion rate of  $6 \times 10^{-5}/\text{h}$  was assumed for temperatures above  $800^\circ\text{C}$  in the previous work [15]. In this work a constant expansion rate of  $-6 \times 10^{-5}/\text{h}$  was assumed for temperatures above  $800^\circ\text{C}$  leading to shrinkage to compare the results to that of the previous study. The depth of the penetration is limited to maximum of 5 mm. The penetration rate is assumed to be 0.05 mm per hour. For now, it

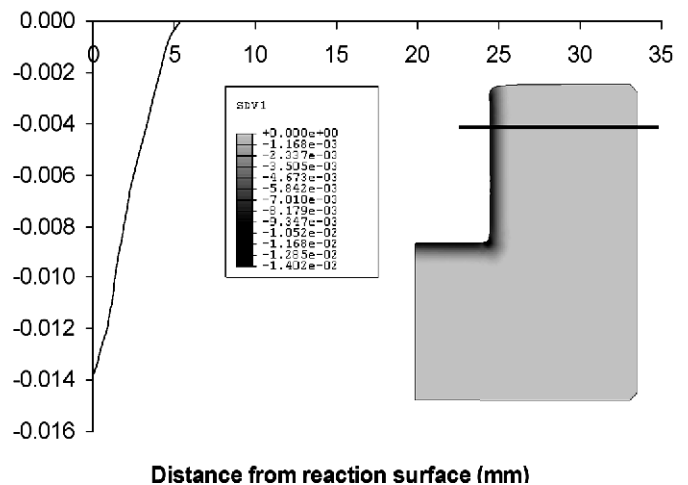


**Figure 4.** Reactive strain pattern and numerical result.

is also assumed that the chemical reaction would not affect other properties of the refractory. However, it can be incorporated into the model when some realistic experimental data on the chemical reaction becomes available.

## RESULTS AND DISCUSSION

The result of reactive strain is shown in **Figure 4**. A thin layer of shrinkage zone which is about 5 mm in thickness is created behind the surface of the hole due to chemical reaction. The curve in the plot is the reactive strain along the dotted line in the contour pattern. Reactive strain is highest on the surface and reduces to zero at the end of the reaction zone. Due to the negative assumption of the reaction rate, value of the shrinkage in this study is fully reversed from the expansion value in the previous study [15].

As a result of the shrinkage in the reaction zone, tensile stress is developed in the same region and causes tensile damage to the material. **Figure 5** shows the predicted tensile damage pattern in the refractory cup after the corrosion test. Compared with the results in the previous study [15], the tensile damage region is almost the same as the compressive damage region in the study of previous study [15]. Tensile damage is highest on the reaction surface, and then decreases toward inside of the cup. As a result, tensile cracking would be caused on the surface instead of spalling when chemical expansion occurs.

**Figure 6** shows the predicted compressive damage in the refractory cup. Due to stress balance, compressive stress is developed at the end of the reaction zone and causes compressive damage in this region. However, the compressive damage region in this study is not reversible from the result of previous study [15]. Unlike the tensile damage region which occurred behind the entire reaction zone in the previous study [15], the compressive damage occurs only in a region close to the top edge of the hole. Because of the significant reactive strain, the chemical reaction dominates the stress and strain development in the refractory cup. When chemical shrinkage happens, the strain and stress distribution and value reverse from the previous study [15]. Similar or larger tensile damage can occur under a tensile stress

which has a similar value as the compressive stress in the previous study [15]. However, due to the compressive strength is much higher than the tensile strength, the compressive damage is much lower when under a stress which has a similar value as the tensile stress in the previous study [15].

**Figure 7** gives the numerical results of the damages in the cup. The curves in the plot are the damages along the dotted line in **Figure 4**. Tensile damage starts from the reaction surface and ends at a depth about 5 mm away from the surface. The maximum compressive damage, which is about 1, is on the surface. Compressive damage occurs just around the end of the reaction zone. The maximum compressive damage, which is about 0.17, is much lower than the maximum tensile damage, and lies right behind the reaction zone. The total damage is dominated by the tensile damage in the reaction zone and by the compressive damage in the remainder of the refractory cup. The total damage zone is smaller than



**Figure 6.** Predicted compressive damage pattern.

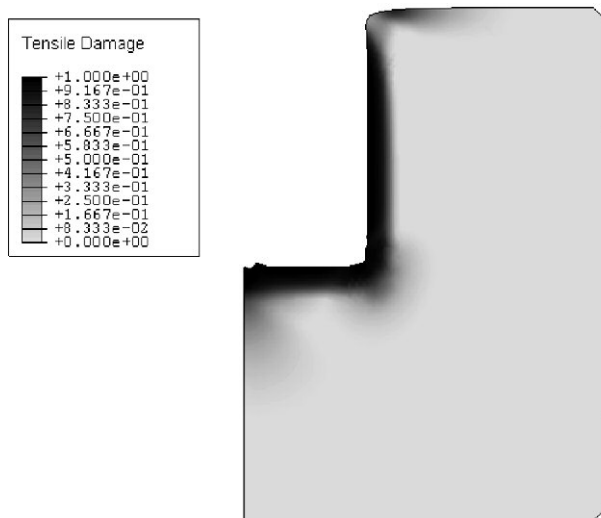


**Figure 5.** Predicted tensile damage pattern.

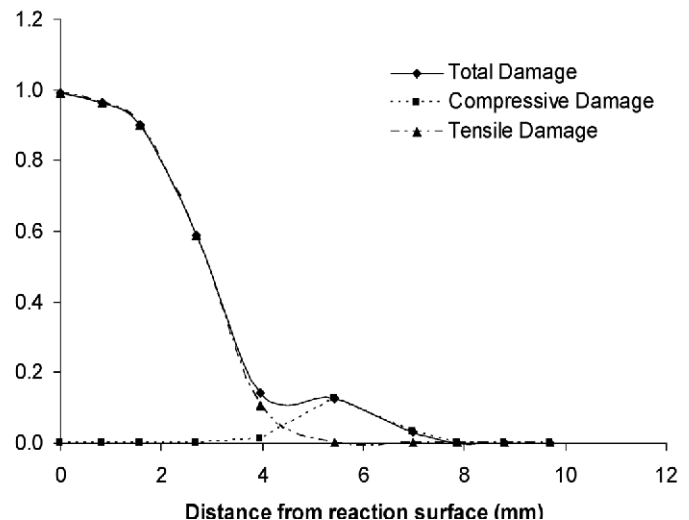


**Figure 7.** Through thickness damage.

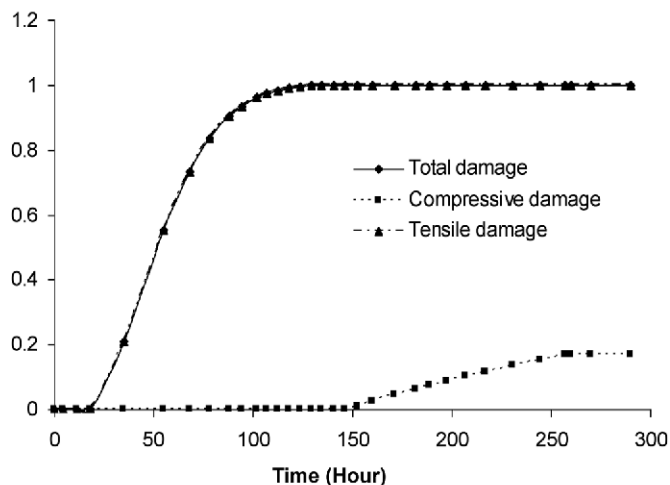


Figure 8. History of the damage.

that in the previous study [15] due to the smaller compressive damage region.

Figure 8 shows the history of the maximum damages. However, the growth of the damages shows nonlinear behavior due to the degradation of the material stiffness. The tensile damage develops earlier and faster than that in the previous study [15], after about 20 hours of the test, and reaches the steady state after about 120 hours. The compressive damage starts long after that in the previous study [15], after about 150 hours of the test. The maximum total damage is dominated by the maximum tensile damage over the entire test.

## CONCLUSIONS


This study presented a CDM based analytical model for predicting the failure behavior of refractory cup experiencing thermal expansion and chemical shrinkage. The reactive strain is almost fully reversed from that in the study with chemical expansion. However, the damage is not fully reversible. Similar or larger tensile damage occurs in the reaction zone rather than compressive damage as in the refractory cup with chemical expansion. Only a very small compressive damage region occurs at the end of the reaction zone. Tensile damage develops earlier and faster than that in the cup with chemical expansion. Compressive damage develops more slowly than that in the cup with chemical expansion. Total damage is dominated by the tensile damage. This work gives a further understanding of the effect of chemical reaction on the failure of the refractory cup. It will help in the development and application of refractories.

## REFERENCES

1. J. Faber and O. S. Verheijen, "Refractory Corrosion under Oxy-Fuel Firing Conditions," *Ceram. Eng. Sci. Proc.*, **18** [1] 109-119, (1997).
2. A. Gupta and S. M. Winder, "Testing Oxy-Fuel Furnace Crown Materials," *Glass*, **73** [7] 260-262, (1996).
3. R. A. Peascoe, J. R. Keiser, C. R. Hubbard, M. P. Brady and J. P. Gorog, "Performance of Selected Materials in Molten Alkali Salts," International Symposium on Corrosion in the Pulp & Paper Industry 2001, 189-200, (2001).
4. C. A. Brown and W. D. Hunter, "Operating Experience at North America's First Commercial Black Liquor Gasification Plant," International Chemical Recovery Conference, Tampa, FL, 655-662, June 1-4, (1998).

5. L. Stigsson, "Chemrec™ Black Liquor Gasification," International Chemical Recovery Conference, Tampa, FL, 663-674, June 1-4, (1998).
6. C. P. Dogan, K. Kwong, J. P. Bennett, R. E. Chinn and C. L. Dahlim, "New Developments in Gasifier Refractories," Gasification Technologies 2002 Conference, San Francisco, CA, October 27-30, (2002).
7. E. Chen and O. Buyukozturk, "Thermomechanical Behavior and Design of Refractory Linings for Slagging Gasifiers," *Am. Ceram. Soc. Bull.*, **64** [7] 988-94 (1985).
8. C. A. Schacht, "Refractory Linings," Marcel Dekker, Inc., (1995).
9. J. Sweeney and M. Cross, "Analyzing the Stress Response of Commercial Refractory Structures in Service at High Temperatures, II. A Thermal Stress Model for Refractory Structures," *Trans. J. Br. Ceram. Soc.*, **81**, 47-52, (1982).
10. O. Buyukozturk and T. Tseng, "Thermomechanical Behavior of Refractory Concrete Lining," *J. Am. Ceram. Soc.*, **65** [6] 301-307, (1982).
11. J. Rawers, J. Kwong, and J. Bennett, "Characterizing Coal-gasifier Slag-refractory Interactions," *Materials at High Temperatures*, **16** [4] 219-222, (1999).
12. E. Chen, "Simulation of the Thermomechanical Behavior of Monolithic Refractory Lining in Coal Gasification Environment," *Radex Rundschau*, **4**, 376-384, (1990).
13. K. Andreev, H. Harmuth, "FEM Simulation of the Thermomechanical Behavior and Failure of Refractories - A Case Study," *J. Mat. Proc. Tech.*, **143-144** [1] 72-77, (2003).
14. S. Yilmaz, "Thermomechanical Modeling for Refractory Lining of a Steel Ladle Lifted by Crane," *Steel Research*, **74** [8] 485-490, (2003).
15. Xiaoting Liang, William L. Headrick, Lokeswarappa R. Dharani, Shuangmei Zhao and Jun Wei, "Failure Analysis of Refractory Cup under Thermal Loading and Chemical Attack Using Continuum Damage Mechanics," UNITECR '05, Orlando, FL, 980-984, Nov. 8-11, (2005).
16. L. M. Kachanov, "Rupture Time under Creep Conditions," *Izv. Acad. Nauk USSR, OTN*, **8**, 26-31, (1958).
17. J. Lemaitre, "A Continuum Damage Mechanics Model for Ductile Fracture," *J. Engrg. Mat. and Technol.*, **107** [1], 83-89, (1985).
18. L. M. Kachanov, "Introduction to Continuum Damage Mechanics," Martinus Nijhoff Publishers, Dordrecht, the Netherlands, (1986).
19. J. L. Chaboche, "Continuum Damage Mechanics, Part I & II," *J. Appl. Mech.*, **55**, 59-72, (1988).
20. A. Hillerborg, M. Modeer and P. E. Petersson, "Analysis of Crack Formation and Crack Growth in Concrete by Means of Fracture Mechanics and Finite Elements," *Cement and Concrete Research*, **6**, 773-782, (1976).
21. J. Lubliner, J. Oliver, S. Oller and E. Oñate, "A Plastic-Damage Model for Concrete," International Journal of Solids and Structures, **25**, 299-329, (1989).
22. J. Lee, and G. L. Fenves, "Plastic-Damage Model for Cyclic Loading of Concrete Structures," *J. Eng. Mech.*, **124** [8], 892-900, (1998).
23. A. Saetta, R. Scotta and R. Vitaliani, "Mechanical Behavior of Concrete Under Physical-Chemical Attacks," *J. Eng. Mech.*, 1100-1109, (1998).
24. S. Zhao, "Modeling of Fracture and Damage in Laminated Automotive Glazing Subjected to Normal Head Impact," Ph.D. Dissertation, University of Missouri-Rolla, (2005)
25. X. Liang, "Analysis of Thermomechanical and Failure Behavior of Refractory Linings in A High Temperature

Black Liquor Gasifier,” Ph.D. Dissertation, University of Missouri-Rolla, (2005)

26. T. Hsu, “The Finite Element Method in Thermomechanics,” Allen & Unwin, Inc., (1986).
27. “ABAQUS/Standard User’s Manual,” Hibbitt, Karlsson & Sorensen, Inc., Vol. 1, Version 6.3.
28. MatWeb.com Database, a Division of Automation Creations, Inc. <http://www.matweb.com>.
29. NIST WebSCD Database, Ceramic division, National Institute of Standards and Technology. <http://www.ceramics.nist.gov>.
30. R. A. Peascoe, J. R. Keiser, C. R. Hubbard, M. P. Brady and J. P. Gorog, “Performance of Selected Materials in Molten Alkali Salts,” International Symposium on Corrosion in the Pulp & Paper Industry 2001, 189-200, (2001). 



The Name.  
The Degree.  
The Difference.

# *Refractories Applications and News* announces the retirement of **Dwight Whittemore**

As many of you already know, Dwight Whittemore retired the end of this past year. He has been a member of our sales staff since April of 2001. He will be missed by all of the staff and we would all like to wish him the very best in his retirement.

**Good Luck and  
Thank You  
for your service!**